Breast Cancer Research

Breast Cancer RESEARCH

This Provisional PDF corresponds to the article as it appeared upon acceptance. Copyedited and fully formatted PDF and full text (HTML) versions will be made available soon.

ABCC5 supports osteoclast formation and promotes breast cancer metastasis to bone

Breast Cancer Research 2012, **14**:R149 doi:10.1186/bcr3361

Anna A Mourskaia (anna.mourskaia@mail.mcgill.ca)
Eitan Amir (eitan.amir@uhn.ca)
Zhifeng Dong (zhifeng.dong@mcgill.ca)
Kerstin Tiedemann (kerstin.tiedemann@mcgill.ca)
Sean Cory (sean.cory@mcgill.ca)
Atilla Omeroglu (atilla.omeroglu@mcgill.ca)
Nicholas Bertos (nicholas.bertos@mcgill.ca)
Veronique Ouellet (veronique.ouellet@mcgill.ca)
Mark Clemons (mclemons@toh.on.ca)
George L Scheffer (GL.Scheffer@vumc.nl)
Morag Park (morag.park@mcgill.ca)
Michael Hallett (hallett@mcb.mcgill.ca)
Svetlana V Komarova (svetlana.komarova@mcgill.ca)
Peter M Siegel (peter.siegel@mcgill.ca)

ISSN 1465-5411

Article type Research article

Submission date 14 July 2012

Acceptance date 12 November 2012

Publication date 22 November 2012

Article URL http://breast-cancer-research.com/content/14/6/R149

This peer-reviewed article can be downloaded, printed and distributed freely for any purposes (see copyright notice below).

Articles in *Breast Cancer Research* are listed in PubMed and archived at PubMed Central.

For information about publishing your research in *Breast Cancer Research* go to

http://breast-cancer-research.com/authors/instructions/

© 2012 Mourskaia *et al.*
This is an open access article distributed under the terms of the Creative Commons Attribution License (http://creativecommons.org/licenses/by/2.0), which permits unrestricted use, distribution, and reproduction in any medium, provided the original work is properly cited.

ABCC5 supports osteoclast formation and promotes breast cancer metastasis to bone

Anna A Mourskaia[1,9], Eitan Amir[10], Zhifeng Dong[1,9], Kerstin Tiedemann[2,3], Sean Cory[4,9], Atilla Omeroglu[5], Nicholas Bertos[6,9], Véronique Ouellet [1,9], Mark Clemons[11], George L Scheffer[12], Morag Park[1,7,9], Michael Hallett[4,9], Svetlana V Komarova[2,3], and Peter M Siegel[1,7,8,9*]

[1]Department of Medicine, McGill University, 1110 Pine Avenue West, Montreal, Quebec, H3A 1A3, Canada.

[2]Faculty of Dentistry, McGill University, 3640 University Street, Montreal, Quebec, H3A 0C7, Canada.

[3]Shriners Hospital for Children, 1529 avenue Cedar, Montreal, Quebec, H3G 1A6, Canada.

[4]Centre for Bioinformatics, McGill University, 3649 Promenade Sir William Osler, Montreal, Quebec, H3G 0B1, Canada.

[5]Department of Pathology, McGill University, 3775 University Street, Montreal, Quebec, H3A 2B4, Canada.

[6]Breast Cancer Functional Genomics Group, McGill University, 1160 Pine Avenue West, Montreal, Quebec, H3A 1A3, Canada.

[7]Department of Biochemistry, McGill University, 3655 Promenade Sir William Osler, Montreal, Quebec, H3G 1Y6, Canada.

[8]Department of Anatomy and Cell Biology, McGill University, 3640 University Street, Montreal, Quebec, H3A 2B2, Canada.

[9]Goodman Cancer Research Centre, McGill University, 1160 Pine Avenue West, Montreal, Quebec, H3A 1A3, Canada.

[10]Division of Medical Oncology, Princess Margaret Hospital, 610 University Avenue, Toronto, Ontario, M5T 2M9, Canada.

[11]Division of Medical Oncology, Ottawa Hospital Cancer Centre, 501 Smyth Road, Ottawa, Ontario, K1H 8L6, Canada.

[12]VU medical center, Department of Pathology, Postbus 7057 1007 MB, Amsterdam, the Netherlands.

[*]Corresponding author: peter.siegel@mcgill.ca

Abstract

Introduction: Bone is the most common site of breast cancer metastasis and complications associated with bone metastases can lead to a significantly decreased patient quality of life. Thus, it is essential to gain a better understanding of the molecular mechanisms that underlie the emergence and growth of breast cancer skeletal metastases.

Methods: To search for novel molecular mediators that influence breast cancer bone metastasis, we generated gene expression profiles from laser capture microdissected trephine biopsies of both breast cancer bone metastases and independent primary breast tumours that metastasized to bone. Bioinformatics analysis identified genes that are differentially expressed in breast cancer bone metastases compared to primary, bone metastatic breast tumours.

Results: ABCC5, an ATP-dependent transporter, was found to be overexpressed in breast cancer osseous metastases relative to primary breast tumours. In addition, ABCC5 was significantly up-regulated in human and mouse breast cancer cell lines with high bone-metastatic potential. Stable knockdown of *ABCC5* substantially reduced bone metastatic burden and osteolytic bone destruction in mice. The decrease in osteolysis was further associated with diminished osteoclast numbers *in vivo*. Finally, conditioned media from breast cancer cells with reduced ABCC5 expression failed to induce *in vitro* osteoclastogenesis to the same extent as conditioned media from breast cancer cells expressing ABCC5.

Conclusions: Our data suggests that ABCC5 functions as a mediator of breast cancer skeletal metastasis. ABCC5 expression in breast cancer cells is important for efficient

osteoclast-mediated bone resorption. Hence, ABCC5 may be a potential therapeutic target for breast cancer bone metastasis.

Introduction

The skeleton is a favored site for breast cancer metastases due to unique features of the bone microenvironment, including the presence of growth factors and cytokines stored within the bone matrix [1]. The emergence of bone metastases disrupts normal bone homeostasis by perturbing interactions between bone-forming osteoblasts and bone-resorbing osteoclasts [2]. Breast cancer metastases in bone have typically been described as osteolytic in nature, which are associated with excessive bone destruction [3]. This ultimate shift towards bone resorption results from the ability of tumour cells, either directly or indirectly, to positively influence osteoclast differentiation and activity [4, 5]. Subsequently, elevated bone resorption releases latent growth factors and cytokines that are stored in the bone matrix, which support tumour cell survival and growth that ultimately lead to further bone destruction [6, 7]. Hence, the crosstalk between breast cancer cells and the bone microenvironment results in a vicious cycle of bone destruction and increased tumour growth in bone.

Breast tumours are heterogeneous and cancer cells with bone-specific metastatic capabilities may pre-exist in the primary tumour. Indeed, gene signatures have been generated that predict whether a primary breast tumour will relapse to bone or visceral sites of metastasis [8]. A Src-related signature has also been proposed to segregate primary breast tumours based on their propensity to relapse to bone [9]. Numerous studies have identified cancer intrinsic factors that allow tumour cells to colonize and thrive in the bone microenvironment. In fact, *in vivo* selected breast cancer populations, isolated from bone metastases, have been used to identify unique functional mediators of bone metastasis [10-13].

These approaches have yielded valuable information regarding mechanisms involved in the spread, colonization and growth of breast cancer cells in bone. However, growing evidence reveals discordance between the expression of specific markers in the primary breast tumour and those in the corresponding bone metastases [14]. Up to 40% of breast cancer patients displayed discordance in hormone receptor expression between the primary tumour and their associated bone metastases [15, 16]. Thus, it is likely that the bone microenvironment plays a considerable role in modulating the gene expression profiles of breast cancer cells in emerging bone metastases. Hence, a number of important mediators of breast cancer skeletal metastasis will undoubtedly be overlooked in the analysis of primary breast tumours or breast cancer cells explanted *ex vivo* from bone metastases.

To circumvent these limitations, we sought novel mediators of skeletal metastasis directly in bone metastatic lesions from breast cancer patients. We applied laser capture microdissection to isolate RNA from both trephine-biopsies of bone metastases and primary breast tumours. Numerous genes were differentially expressed between primary breast tumours that later relapsed to bone and breast cancer bone metastases, including several members of the ATP-binding cassette (ABC) transporter family that were overexpressed in the bone metastases relative to primary tumours. ABCC5 was found to be functionally involved in the formation of breast cancer bone metastases in two independent cell-based models.

Materials and methods

Primary Breast Tumour and Bone Metastases

Unguided or CT-guided trephine biopsies were performed on breast cancer patients with known bone involvement at the Princess Margaret Hospital (Toronto, Canada), as previously described [17]. Biopsy material was immediately flash frozen and embedded in OCT compound. All procedures were performed with approval from the Research Ethics Board at the Princess Margaret Hospital. Primary breast tumour material was collected from patients who underwent surgery at the Montreal General or Royal Victoria hospitals (Montreal, Canada). Tumour banking was performed with approval from the Research Ethics Board of the McGill University Health Centre under the protocols SDR-99-780 and SDR-00-966. All patients provided written and informed consent.

Laser Capture Microdissection

Histological sections of primary breast tumours or bone metastases were stained with H&E and examined by a clinical pathologist to identify regions within each section suitable for laser capture microdissection (LCM). Sections (10μm) were stained and dehydrated using a HistoGene LCM Frozen Section Staining Kit (Cat. #: KIT0401, Applied Biosystems). Clusters of invasive mammary epithelial cells were identified and selected using an ArcturusXT Microdissection System powered by ArcturusXT software v.1.1 (Applied Biosystems). Breast cancer cells were captured using an infrared laser adjusted to a diameter of 20μm, laser power set to 65mW and a duration of 20msec and

was pulsed through CapSure HS LCM Caps (Cat. #: LCM0214, Applied Biosystems). The beam was passed over the sample to be collected with an overlap of 30% for each specimen. RNA was extracted from the microdissected cells using a PicoPure RNA Extraction Kit (Cat. #: KIT0204, Applied Biosystems) according to the manufacturer's instructions. RNA integrity and quantity was evaluated using a 2100 Bioanalyzer platform (Agilent Technologies).

RNA Amplification, Labeling, and Hybridization to Agilent Microarray Chips

Total RNA (1-2.5ng) from microdissected material was subjected to two rounds of linear amplification using a RiboAmp HS^{Plus} Amplification Kit (Cat. #: KIT0525, Applied Biosystems), following the manufacturer's protocol. Profiles of resulting amplified RNA (aRNA) were assessed using a 2100 Bioanalyzer (Agilent Technologies). The aRNA samples (5µg) were conjugated to Cy3 dye using an Arcturus Turbo Labeling Kit (Cat. #: KIT0609, Applied Biosystems). Universal human reference RNA (Stratagene) was amplified using the same procedure and labeled with Cy5 dye (CAT # KIT0619, Applied Biosystems). RNA concentration and dye incorporation was measured using a Nanodrop ND-1000 UV-VIS spectrophotometer. Labeled RNA (0.825µg) was then hybridized to 44K whole human genome microarray gene expression chips (Cat. #: G4112F, Agilent Technologies) using a Gene Expression Hybridization Kit (Cat. #: 5188-5242, Agilent Technologies) at 65^{o}C for 17 hours according to the manufacturer's instructions. Microarray chips were washed, dried and immediately scanned on a Microarray Scanner Model G2505B (Agilent Technologies) using Agilent Scanner Control Software vA7.0.1 (Agilent Technologies).

Gene expression analysis

Microarray data were extracted using Feature Extraction Software v. 9.5.3.1 (Agilent Technologies). The raw data were then normalized and differential expression was performed using the LIMMA package in R/bioconductor [18]. Specifically, the arrays were normalized using normexp background correction, loess within array and quantile between array normalization. The p-values for differential expression were adjusted for multiple testing. Candidate gene lists were generated by filtering the data on the basis of > 2-fold difference in expression between bone metastases and primary breast tumours. The microarray data can be accessed through the GEO repository (ID GSE39494) [19].

Real-Time Quantitative Reverse Transcription PCR

RNA obtained following two rounds of amplification was quantified using Quant-iT™ RiboGreen® RNA Reagent based on the manufacturer's protocol (Cat. #: R11491, Invitrogen). Total RNA (25ng) was converted to cDNA using a Transcriptor Reverse Transcriptase kit (Cat. #: 048970300001, Roche) in accordance with the manufacturer's protocol. Following reverse transcription, samples were subjected to real-time PCR analysis employing SYBR Green PCR Master Mix (Cat. #: 04887352001, Roche). Primers were designed using OligoPerfect software (Invitrogen) in the region of the target gene surrounding the Agilent probes and used at a concentration of 0.5μM. Polymerase chain reactions were performed on a LightCycler 480 system (Roche) under the following conditions: pre-incubation step (95^{o}C for 10 min.), 45-cycle amplification sequence (95^{o}C for 10 sec, 53^{o}C for 10 sec, 95^{o}C for 6 sec) and a melting step (95^{o}C for 5sec, 65^{o}C for 1min). A complete list of primer sequences can be found in the

Supplementary Information. Results were analyzed by the absolute quantification method using the second derivative maximum method feature of LightCycler® 480 Software v.1.5.0 SP4 (Roche).

Immunohistochemistry

OCT-embedded primary breast tumours and bone trephine biopsies were sectioned (10μm) and fixed in 2% paraformaldehyde. The sections were blocked with 2% BSA and 5% normal goat serum (NGS) and subsequently incubated overnight at 4^{o}C with a primary antibody directed against ABCC5 (1:25, clone M5I-10). This monoclonal antibody was generated in Dr. Scheffer's laboratory (Amsterdam, the Netherlands) following injection of a bacterial fusion protein containing the N-terminal region of mouse ABCC5. The antibody recognizes mouse ABCC5 but also reacts strongly with the human orthologue. The sections were then incubated with Biotin conjugated secondary antibody and developed with 3-3-diaminobenzidine-tetrahydrochloride (DAB). A standard hematoxylin counterstain was performed to demarcate cellular nuclei.

Primary mammary tumours and hindlimbs were excised from mice and fixed overnight in 4% paraformaldehyde. Bones were decalcified in a solution of 14.5% ethylenediaminetetraacetic acid (EDTA) and 15% glycerol for 4 weeks. Tissues were then paraffin embedded and sectioned. Sections (5μm) were deparaffinized and stained with a freshly prepared tartrate resistant acid phosphatase (TRAP) staining solution (napthol AS-TR Phosphate, fast blue RR salt and sodium tartrate). Slides were scanned using a Scanscope XT digital slide scanner (Aperio, Vista, CA, USA) and analyzed with Imagescope software (Aperio). The number of TRAP positive cells within breast cancer

lesions in bone was counted manually and is presented as the number of osteoclasts per square millimeter of tumour mass.

Immunoblotting

Human and mouse cell lines were lysed in TNE lysis buffer as previously described [20]. Total protein concentrations were determined by Bradford Protein Assay (Cat. #: 500-006, Bio-Rad Laboratories) and 20-50μg of protein were separated by sodium dodecyl sulfate polyacrylamide gel electrophoresis (SDS-PAGE) and transferred to polyvinylidene fluoride (PVDF) membranes (Cat. #: IPVH00010, Millipore). The membranes were blocked in 5% w/v nonfat dry milk containing 0.1% Tween and incubated with the following primary antibodies: ABCC5 (1:100 dilution; M5I-10) and α-tubulin (1:20,000 dilution; Cat. #: T9026, Sigma). The blots were then incubated with horseradish-peroxidase-conjugated secondary antibodies and proteins were visualized with an enhanced chemiluminescence detection system (Cat. #: 34080, Pierce).

DNA constructs

Short hairpin RNA (shRNA) sequences targeting the human and mouse *ABCC5* mRNA, as well as the scrambled control sequence, were designed using the RNAi central website at Cold Spring Harbor Laboratories [21]. The sequences of the shRNAs used for *ABCC5* knockdown are as follows (target sequence denoted in bold text: h = human; m = mouse): *hABCC5* sh: TGC TGT TGA CAG TGA GCG **ACC TCA AAG TCT GCA ACT TTA A**TA GTG AAG CCA CAG ATG TAT TAA AGT TGC AGA CTT TGA GGG TGC CTA CTG CCT GGA; *mabcc5* sh1: TGC TGT TGA CAG TGA GCG **ACC TCA TCC TGT CCT GCT GAA A**TA GTG AAG CCA CAG ATG TAT TTC AGC

AGG ACA GGA TGA GGG TGC CTA CTG CCT CGG A; *mabcc5* sh2: TGC TGT TGA CAG TGA GCG **CCC TGA CTA TGG CAT TCA AGA A**TA GTG AAG CCA CAG ATG TAT TCT TGA ATG CCA TAG TCA GGA TGC CTA CTG CCT CGG A; scrambled sh: TGC TGT TGA CAG TGA GCG **AAG TCC ATA CTT AGT CGA TAG A**TA GTG AAG CCA CAG ATG TAT CTA TCG ACT AAG TAT GGA CTC TGC CTA CTG CCT CGG A. These sequences were PCR amplified, digested and cloned into the LMP vector as *Xho*I/*Eco*RI fragments following published instructions [22].

Cell culture and *in vitro* osteoclastogenesis assay

Parental MDA-MB-231 breast cancer cells were obtained from the American Type Culture Collection and transduced with a triple reporter system as previously described [23]. The MDA-MB-231-derived bone metastatic (1833-BM1) and lung metastatic (4175-LM2) populations were derived as described previously [10, 24]. Human breast cancer cell lines were cultured in DMEM supplemented with 10% fetal bovine serum and MEM Nonessential Amino Acids (1X), gentamycin and amphotericin B. The 4T1 murine mammary carcinoma cell line was obtained from the American Type Culture Collection. Non-metastatic 67NR and lung-metastatic 66cl4 murine mammary carcinoma cell lines [25] were kindly provided by Dr. Fred Miller (Barbara Ann Karmanos Cancer Institute, Detroit, MI) and cultured in DMEM supplemented with 10% fetal bovine serum, 10 mmol/L HEPES, 1 mmol/L sodium pyruvate, 1.5 g/L sodium bicarbonate, gentamycin and amphotericin B.

For the *in vitro* osteoclastogenesis assay, $5x10^5$ 4T1-derivative cells were plated in 10cm cell culture dishes. The following day, media was changed to DMEM supplemented with 10% fetal bovine serum and subsequently conditioned for 48 hours. Protocols used to establish primary osteoclast cultures from BALB/c mice were performed in accordance with the McGill University guidelines established by the Canadian Council on Animal Care. Bone marrow was collected from tibiae and femurs of mice (BALB/c, male, 6 weeks old, Charles River) as described previously [26] and cultured in 75-cm^2 tissue culture flasks ($15x10^6$ cells per flask) in α-minimal essential medium supplemented with 10% fetal calf serum, penicillin, streptomycin and 25 ng/ml of human recombinant macrophage-colony stimulating (M-CSF) factor (Cat. #: 300-25, PeproTech Inc.). On day 1, non-adherent cells were collected, plated at $5x10^3$ cells/cm^2, and supplemented with M-CSF (50 ng/ml) and recombinant GST-RANKL (100 ng/ml). On day 4, fresh media with or without RANKL (100 ng/ml) or conditioned media harvested from 4T1-derivatives (10%) were added to the cultures. M-CSF (50 ng/ml) was present in all conditions tested. On day 6, cells were fixed with 4% paraformaldehyde (10 min), washed with phosphate-buffered saline, and stained for tartrate-resistant acid phosphatase (TRAP) (Cat. #: 387A-KT, Sigma).

Left cardiac ventricle injections

Female SCID/beige and BALB/c mice (4-6 weeks) were purchased from Charles River Laboratories. The animals were housed in facilities managed by the McGill University Animal Resources Centre. All animal experiments were conducted under a McGill University approved Animal Use Protocol in accordance with guidelines established by the Canadian Council on Animal Care. Breast cancer cells were harvested

from sub-confluent cultures and resuspended in sterile PBS. Mice were anaesthetized with isofluorane and $1x10^5$ of human or mouse breast cancer cells, in a volume of 100µl, were injected into the left cardiac ventricle using 26G needles [12]. A successful injection was distinguished by the pumping of arterial blood into the syringe during the injection procedure and confirmed by a uniform luminescent signal throughout the entire animal body post 1833-BM1 cell inoculation.

In vivo bioluminescent imaging

Tumour outgrowth within skeletal sites of mice injected with 1833-BM1 breast cancer cells was monitored using an IVIS 100 (Caliper Life Sciences) bioluminescence imaging system as previously described [27]. The resulting data were normalized to the signal generated by the initial cell inoculum, which was measured immediately post cardiac injection. Total metastatic burden was measured by setting a uniform scale for each group of mice, outlining regions of interest around all luminescence signals in the body and summing them.

X-ray micro-computed tomography (µCT) imaging

At the endpoint of the cardiac injection experiments (21 days for 1833-BM1 and 13 days for the 4T1 models) mice were anaesthetized and immobilized with tape in the imaging tube of a Skyscan 1178 µCT. All images were obtained with an X-ray source operating at 50kV (1833-BM1) or 45kV (4T1) and 615mA with an exposure time of 480 msec. Animals were rotated through 180^o at a rotation step of 1.26^o (1833-BM1 cells) and 0.9^o (4T1 cells). Cross-section images from tomography projection images were reconstructed using the NRecon program package v.1.6.4.7 (SkyScan). Reconstruction

parameters, including smoothing (1), ring artefacts reduction (4) and beam-hardening correction (30%) were fixed for all the samples. The dynamic image range was defined between 0 and 0.045 for all the samples. Bone alignment was adjusted in all specimens using DataViewer v.1.4.3.2 (SkyScan). Bone volume was determined in 3D using CTAn software v.1.11.8.0 (SkyScan). Briefly, for each bone a volume of interest (VOI) was determined starting under the growth plate and extending 20 (femur) and 25 (tibia) sections below the diaphysis. For each model, the VOI was designed by drawing user-defined polygons on the 2D sections that encompass the bone of interest. In the binary image mode, the histogram was set at minimum 100 to maximum 255 for a given dataset for each specimen. Each 3D model was visualized using CTvox v.2.3 (SkyScan). The absolute bone volume was determined for each piece of bone and expressed in cubic millimeters. Control groups, including uninjected mice of similar strain and age as the experimental animals, were used as reference for normal bone volume. The degree of bone destruction was determined as percentage difference between the average bone volumes in experimental groups compared to those in the appropriate control cohorts.

Statistical analysis

Statistical significance values for RT-qPCR expression, whole body luminescence, μCT bone volumes and osteoclast assays were obtained by performing a two-sample variance two-tailed Student's t-test.

Supplemental Materials and Methods can be found as Additional file 1.

Results

Laser Capture Microdissection of Human Breast Cancer Bone Metastases

To generate gene expression profiles of primary human breast cancer bone metastases and primary breast cancers, we selected 5 fresh frozen samples for each group (Additional file 2, Additional file 3). For this study, the primary breast tumours were not patient-matched to the bone metastases.

The bone metastases were obtained from breast cancer patients that had consented to undergo unguided or CT-guided trephine biopsies. To ensure that the biopsy material contained breast cancer cells, we performed co-immunofluorescence staining with both luminal (CK8/18) and basal (CK5) cytokeratins. Clusters of CK5-positive epithelial cells were found in all of the bone metastases used in our analysis, a marker associated with basal-like breast cancer cells (Additional file 4, *top panels*). However, in three out of five samples (BM-001, BB-005, BM-007), expression of the luminal cytokeratin 8/18 markers were also detected, suggesting that these breast cancer cells were of mixed lineage (Additional file 4, *middle panels*). A DAPI stain identified the location of all cells in each section (Additional file 4, *bottom panels*).

Clusters of invasive epithelial cells were specifically identified in each sample and subjected to laser capture microdissection (LCM) (Figure 1). Following RNA extraction, two rounds of amplification and labeling, gene expression profiles of each sample were obtained using human whole genome (44K) Agilent microarray chips. Unsupervised clustering using the top 200 most variable probes segregated the samples into primary

breast tumours and bone metastases, irrespective of ER, PR and Her2 status (data not shown).

Identification of putative molecular mediators of breast cancer skeletal metastasis

Filtering the differential gene expression data yielded a list of 244 overexpressed and 185 under-expressed probes in breast cancer skeletal metastases compared to primary breast tumours. Following a review of the literature, 118 up-regulated and 82 down-regulated unique genes with known or ascribed functions were identified in bone metastases compared to primary tumours (Additional file 5). These genes were further categorized into distinct functional groups based on their proposed roles, which included mediators of: transcription, translation, post-translational modification, mitochondrial functions/metabolism, cell cycle progression, cellular transport, cytoskeletal organization, cellular adhesion/migration/invasion, tumour microenvironment, chemotaxis, cell differentiation, apoptosis/survival and other (Additional file 6).

A number of genes responsible for cellular migration and invasiveness were down regulated in bone metastases compared to primary tumours (*NCK2* [28], *PHPT1* [29], *LIMK1* [30], *TESK1* [31], *TMSB10* [32]). Moreover, a few genes involved in modulation of the extracellular matrix (*ADAMTS4* [33], *MMP1* [34], *MMP3* [35] and angiogenesis (*MFAP5* [36], *SFRP2* [37], *SRPK1* [38], *VEGF* [39], *CHI3L1* [40]) were found to be expressed at higher levels in the primary breast tumours compared to the bone metastases. Our data supports a role for these two gene sets in promoting local invasion at the primary tumour, which may have facilitated breast cancer dissemination to distant organs such as the bone.

Interestingly, the expression of genes (*GFRA1*, *ID1, ABCG2*) implicated in the regulation of hematopoietic progenitor cells was found to be elevated in bone metastases compared to the primary breast tumours that had relapsed to bone [41-44]. This finding lends support to the notion that breast cancer cells may utilize the endosteal niche, which pre-exists within the bone microenvironment, to colonize the bone [45]. It has been reported that cancer cells potentially compete with HSCs for occupancy of these endosteal niches and represent privileged sites where cancer cells first establish [46]. Additionally, a number of pro-survival (*BCL2* [47], *PPEF2* [48]) and pro-apoptosis (*BID* [49], *HEBP2* [50], *PKNOX1* [51]) genes were up- and down-regulated, respectively, in bone metastases compared to primary breast tumours. Importantly, the expression of well-known pro- (*BCL2*) and anti-apoptotic (*BID*) genes was validated by RT-qPCR (Additional file 7, Additional file 8). Finally, macrophage inhibitory factor (*MIF*) was found to be down-regulated in breast cancer skeletal metastases compared to the primary mammary tumours. It has been shown that MIF promotes breast cancer cell proliferation [52, 53], angiogenesis [54] and survival [55]. However, though MIF was frequently over-expressed in primary mammary tumour tissues its presence was inversely correlated with the nodal spread of breast cancer [56]. A recent study has suggested that intracellular MIF levels are low in aggressive breast cancer cell lines and that cytosolic MIF expression associates with an increased recurrence-free survival patients, whereas extracellular MIF promotes migration and invasion of breast cancer cells [57]. Interestingly, MIF was also shown to inhibit osteoclastogenesis in *in vitro* and *in vivo* assays [58]. Thus, loss of MIF may be required during the formation of osteolytic bone metastases.

Using RT-qPCR analysis, we were able to validate the gene expression changes for several candidates initially identified via microarray-based gene expression profiling (Additional file 7, Additional file 8). Intriguingly, several members of the ATP-binding cassette (ABC) transporter superfamily (*ABCA5*, *ABCC5* and *ABCG2*) were consistently overexpressed in breast cancer bone metastases compared to primary breast tumours (Additional file 7, Additional file 8). While a significant body of literature has linked ABCG2 expression with drug resistance in breast cancer [59], considerably less is known about ABCA5 and ABCC5 in this disease.

ABCC5 is overexpressed in breast cancer bone metastases and bone metastatic breast cancer cells

Given the availability of antibody reagents, we focused our attention on *ABCC5*, a candidate gene that was found to be significantly overexpressed in breast cancer skeletal metastases relative to primary tumours by both microarray-based and RT-qPCR methods (Figure 2A). Furthermore, immunohistochemical analysis revealed that ABCC5 protein levels appeared to be enriched in breast cancer bone metastases compared to primary mammary tumours (Figure 2B).

As a first step to functionally validate a role for ABCC5 in promoting bone metastasis, we interrogated the expression of ABCC5 in breast cancer cell lines with high bone metastatic potential. Using a series of *in vivo* selected MDA-MB-231 breast cancer cell populations that are metastatic to bone and lung, we demonstrate that ABCC5 expression was highest in bone metastatic cell populations (1833-BM1) when compared to lung metastatic cells (4175-LM2) or the parental MDA-MB-231 cell line (Figure 3A).

We also examined an independent murine breast cancer series isolated from the same original mammary tumour that are either non-metastatic (67NR), lung-metastatic (66cl4) or metastatic to multiple organs, including bone (4T1). We demonstrate that ABCC5 expression was considerably higher in the bone metastatic 4T1 cell line relative to lung metastatic 66cl4 and non-metastatic 67NR populations (Figure 4A).

Loss of ABCC5 expression diminishes the formation of breast cancer bone metastases

To determine if ABCC5 is important for the ability of breast cancer cells to metastasize to bone, we stably diminished ABCC5 expression in bone-metastatic breast cancer cell lines using short hairpin RNAs (shRNA). An efficient and stable knockdown was achieved in both human 1833-BM1 (Figure 3B) and mouse 4T1 (Figure 4B) breast cancer cell lines relative to the parental cell lines or populations harboring a scrambled shRNA control. Importantly, diminished ABCC5 expression in human and mouse mammary cancer cell lines did not affect their proliferative properties *in vitro* or their *in vivo* growth as mammary tumours (Additional file 9). However, loss of ABCC5 expression in the human 1833-BM1 population resulted in a 4-fold reduction in overall bone metastatic burden following left cardiac ventricle injections, as measured by bioluminescence imaging (Figure 3C). While the total number of bone metastases/mouse was similar in scrambled control and *ABCC5* shRNA cohorts (Figure 3D), the size of the individual lesions was clearly diminished (Figure 3C). Interestingly, the osteolytic bone metastatic lesions arising in mice injected with ABCC5^{low} 1833-BM1 cells were significantly smaller (6% bone destruction) than those observed in animals injected with

the scrambled shRNA-expressing population (16% bone destruction), as measured by volumetric μCT analysis (Figure 3E).

To confirm this functional role for ABCC5 in promoting breast cancer metastasis to bone, we analyzed the effects of reduced ABCC5 expression on the ability of 4T1 breast cancer cells to form bone metastases following cardiac injection. Two independent 4T1 populations, each harboring a unique shRNA targeting *ABCC5*, and 4T1 cells containing a scrambled shRNA were injected into separate cohorts of mice. Similar to our results with the human breast cancer cell line model, suppression of ABCC5 expression in mouse breast cancer cell lines did not result in the alteration of total number of bone metastases/mouse (Figure 4C). However, μCT analysis revealed that reduced *ABCC5* expression in mouse derived 4T1 cells resulted in significantly less (shRNA #1: 26% bone destruction; shRNA#2: 16% bone destruction) bone destruction compared to the scrambled controls (40% bone destruction) (Figure 4D). Interestingly, there was no difference in either the number of spontaneous lung metastases or the size of the lesions formed by 4T1 derivative breast cancer cells harboring the ABCC5 knockdown when compared to cells expressing the scrambled shRNA (Additional file 10). Together, these results support an important functional role for ABCC5 in promoting the colonization and growth of breast cancer cells specifically within the bone.

Proliferation and apoptosis are not affected in mammary tumours or bone metastases by diminished ABCC5 expression

To investigate potential explanations for the reduction in the size of osteolytic lesions arising in mice injected with breast cancer cells engineered to express ABCC5 shRNAs,

we examined the proliferative and apoptotic indices in both mammary tumours and bone metastases. In agreement with the observation that reduced ABCC5 levels did not negatively influence primary tumour growth (Additional file 9), we did not observe statistically significant differences in the percentage of Ki67-positive nuclei in primary tumours derived from 1833-BM1 or 4T1 cells, possessing normal or shRNA-reduced levels of ABCC5 (Additional file 11A and B). Interestingly, no differences in proliferation were observed in bone metastases that formed in mice injected with 1833-BM1 or 4T1 derived breast cancer populations, which possessed diminished ABCC5 expression or normal endogenous levels of ABCC5 (Additional file 11C and D).

To determine whether loss of ABCC5 was associated with elevated levels of apoptosis, we performed immunohistochemical staining for cleaved caspase-3 in both mammary tumours and bone metastases that arose in mice injected with 1833-BM1 or 4T1 derived breast cancer populations. Diminished ABCC5 expression did not result in elevated apoptosis in either end-stage mammary tumours (Additional file 12A and B) or end-stage osteolytic bone metastases (Additional file 12C and D).

Reduced ABCC5 levels in breast cancer cells correlate with reduced osteoclast numbers within bone metastatic lesions and diminished *in vitro* osteoclastogenesis

To better define the mechanisms responsible for impaired bone metastasis in mice injected with the *ABCC5* knockdown breast cancer cell populations, we examined the density of osteoclasts present within lytic lesions formed by the MDA-MB-231 and 4T1-derived cells. Representative bone sections were stained for tartrate resistant acid phosphatase (TRAP), an osteoclast-specific marker. The number of TRAP-positive cells

was significantly reduced by 2.7 times in the 1833-BM1 lesions expressing the *ABCC5* shRNA compared to the bone metastases harbouring the scrambled shRNA control (Figure 5A). Two independent 4T1-derived populations, each expressing a unique shRNA targeting *abcc5*, also showed a 1.8 and 4.1-fold reduction in TRAP-positive cells when compared to 4T1 breast cancer cells harbouring the scrambled shRNA control (Figure 5B). Together, these data demonstrate that loss of ABCC5 function in breast cancer cells results in decreased osteoclast numbers within bone metastatic lesions. These results are in agreement with the diminished capacity to form osteolytic metastases that is exhibited by breast cancer cells with diminished ABCC5 expression. Our data support a role for ABCC5 in promoting the specific growth of breast cancer cells within the bone microenvironment through a mechanism that favours osteoclast formation and/or function.

To further investigate the potential role of tumour intrinsic ABCC5 in promoting osteolytic lesion formation, we performed an *in vitro* osteoclast differentiation assay. Primary osteoclast cultures were established from murine bone marrow and primed with macrophage colony-stimulating factor (M-CSF) and receptor activator of nuclear factor κ-B ligand (RANKL). The osteoclast precursors were subsequently stimulated with conditioned media from the 4T1-derived populations, which exhibited the most pronounced difference in osteoclast numbers between control and ABCC5 knockdown breast cancer cells *in vivo* (Figure 5). Intriguingly, the number of multinucleated TRAP-positive osteoclasts was reduced by 1.3 and 1.6 times when osteoclast precursors were cultured in media collected from 4T1 harbouring two independent *abcc5*-specific shRNAs, when compared to the scrambled shRNA control (Figure 6).

Discussion

The vicious cycle of bone metastasis formation argues that breast cancer cells colonizing the bone are influenced by growth factors that are stored in the bone matrix, which are released during bone resorption [1, 2]. These influences predict that breast cancer bone metastases will differ in their gene expression profiles from primary breast tumours. To evaluate gene expression profiles of *in situ* bone metastases from breast cancer patients, we have performed laser capture microdissection (LCM) on trephine biopsies and compared them to profiles obtained from LCM material of primary breast tumours. Numerous genes were differentially expressed between primary breast tumours with known relapse to bone versus breast cancer bone metastases and were categorized according to their known or proposed functions.

Intriguingly, three members of the ATP-binding cassette (ABC) transporter family (*ABCA5, ABCC5, ABCG2*) were overexpressed in breast cancer bone metastases compared to primary tumours that are metastatic to bone (Additional file 7, Additional file 8). The human genome encodes 49 ABC genes that are arranged in seven subfamilies designated A to G [60]. These genes encode ATP energy dependent molecular pumps that transport substrates across membranes, either in or out of cells or into cellular vesicles, against their electrochemical gradient [61]. Consistent with the role of these transporters in the excretion of diverse compounds, their expression (ABCG2, ABCA1, ABCA7, ABCG1, ABCG5) has been found in lactating mammary epithelium [62, 63]. Furthermore, the ABC transporters (ABCG2, ABCB1) have been proposed to be

expressed by quiescent cancer stem cells, which allows them to survive cytotoxic or targeted therapies leading to relapse [64].

We focused on ABCC5 (MRP5) as a candidate mediator of breast cancer skeletal metastases due to the fact that we validated its expression in bone metastases at both the mRNA and protein level (Figure 2). ABCC5 represents a membrane spanning protein belonging to the C subfamily of the ABC transporters, with the ability to transport endogenous cyclic nucleotides [65]. One concern associated with our identification of ABC transporters was the possibility that these proteins were up-regulated as a consequence of the patient's treatment history rather than any specific role that they might play in the establishment of bone metastases [66, 67]. To address this possibility, we examined ABCC5 expression in breast cancer cell populations that exhibit a bone metastatic phenotype. We first employed a series of *in vivo* selected MDA-MB-231 cell lines with different organ-specific metastatic potential and found that ABCC5 was most highly expressed in the bone metastatic MDA-MB-231 cells when compared to the parental and lung-tropic MDA-MB-231 cells (Figure 3A). We next determined the level of ABCC5 expression in mouse-derived breast cancer cells with differential metastatic abilities. Consistent with the result in MDA-MB-231 cells, the highly metastatic 4T1 population, which is highly metastatic to bone and other sites, exhibited considerably higher ABCC5 expression in comparison with lung-only metastatic 66cl4 and non-metastatic 67NR populations (Figure 4A). These data reveal that ABCC5 expression is highest in breast cancer cells that display enhanced bone metastatic phenotypes, under conditions where no treatments (anti-estrogens, chemotherapy or bisphosphonates) were employed. Thus, it is conceivable that elevated ABCC5 expression is selected for due to a

particular function that enables breast cancer cells to efficiently colonize the bone microenvironment.

The physiological functions of ABCC5 are, at present, poorly defined. It was reported that this protein serves as an efflux pump for intracellular cyclic guanosine monophosphate (cGMP) and, to a lesser degree, cyclic adenosine monophosphate (cAMP) [65]. A growing body of literature suggests that elevated intracellular cGMP levels results in reduced breast cancer cell proliferation, ultimately triggering apoptosis via activation of Protein Kinase G (PKG) [68-70]. Nitric oxide and naturetic peptides, which serve as activators of soluble and transmembrane guanylyl cyclases respectively, are abundant in bone and exert complex effects on bone cells, bone turnover and bone formation [71]. Thus, we reasoned that up-regulation of a cGMP efflux pump could be advantageous for breast cancer growth and survival in the bone microenvironment. Indeed, diminished ABCC5 expression resulted in a significant reduction in the size of osteolytic lesions formed by both 1833 and 4T1 breast cancer cell models when compared to controls. However, this reduction was not a reflection of general alterations in breast tumour cell growth (Additional file 9). Consistently, there was no change in breast cancer cell proliferation, in either primary breast tumours or bone metastases, when ABCC5 was knocked down compared to controls (Additional file 11). Moreover, the removal of ABCC5 did not result in elevated rates of apoptosis in either primary tumours nor in breast cancer bone metastases, as assessed by immunostaining for cleaved Caspase-3 (Additional file 12). Finally, we did not observe any differences in breast cancer cell apoptosis in response to a stimulator of cGMP production (A-350619 hydrochloride) in control or ABCC5 knock-down cells (data not shown). These

observations suggest that ABCC5 does not promote breast cancer proliferation and survival in end-stage bone metastases through a mechanism that involves cGMP efflux and reduced PKG activation.

Elevated cGMP levels have also been shown to modulate the expression of matrix metalloproteinases (MMPs), although this regulation appears complex. Some studies suggest that elevated cGMP levels can induce the expression of MMP-2 and MMP-9 [72, 73] while others argue that MMP-9 expression or secretion is suppressed by increasing cGMP concentrations [74, 75]. Whether breast cancer cells that express ABCC5, and thus maintain low cytoplasmic cGMP levels through active efflux, are associated with elevated MMP-9 expression or secretion requires further investigation.

One interesting result was the observation that the density of TRAP-positive osteoclasts were reduced in lesions formed by breast cancer cells harbouring reduced ABCC5 levels compared to bone metastases arising from control cells. Consistent with these observations, conditioned media from ABCC5 knockdown cells was less efficient in inducing *in vitro* osteoclast differentiation compared to media collected from cells harbouring scrambled shRNA. It should be noted that the diminishment of osteoclastogenesis was not complete, and in the case of one ABCC5 shRNA (shRNA#1) only trended towards a decrease in ostoclastogenesis. These results raise the possibility that the substrate of ABCC5 might directly influence osteoclast differentiation; however, it is also conceivable that the cargo that is pumped out of breast cancer cells by ABCC5 indirectly influences osteoclastogenesis through an intermediate cell type present in the bone microenvironment.

Previous studies have shown that high levels of cGMP can negatively regulate the ability of osteoclasts to resorb bone disrupting their attachment to the bone surface and preventing efficient secretion of HCl [76, 77]. However, an important phase of the bone resorption mediated by osteoclasts is their ability to break the sealing zone, detach from the bone surface and migrate to a new area of bone and re-initiate bone resorption. Indeed, nitric oxide or cGMP analogs have been shown to stimulate osteoclast migration [78]. Thus, it is conceivable that locally elevated levels of cGMP, by virtue of a growing breast cancer metastasis, could contribute to enhanced osteoclast migration. The reduction of ABCC5 could diminish cGMP efflux, leading to impaired osteoclast motility and decreased bone resorption. This hypothesis might explain the specific requirement for ABCC5 expression in breast cancer cells that metastasize to the bone. Alternatively, an as yet unidentified ABCC5 cargo may be responsible for enhanced osteoclast differentiation and motility that leads to the formation of osteolytic breast cancer metastases in bone.

Conclusions

In conclusion, we have identified ABCC5 as a gene that is overexpressed in breast cancer bone metastases compared to primary breast tumours. This protein was also highly expressed in human and mouse cells breast cancer cell lines that are highly metastatic to bone. Finally, ABCC5 was functionally validated in *in vivo* models to be an important mediator in breast cancer outgrowth in this organ. ABCC5 functions to promote osteolytic bone destruction through the recruitment and enhanced formation of

osteoclasts. Hence, ABCC5 is a novel candidate mediator of breast cancer bone metastasis, which may be a potential target for the development of treatment for this detrimental disease.

Abbreviations

ABC transporter: ATP-binding cassette transporter; aRNA: amplified RNA; cAMP: cyclic adenosine monophosphate; cDNA: complementary DNA; cGMP: cyclic guanosine monophosphate; CK: cytokeratin; EDTA: ethylenediaminetetraacetic acid; IHC: immunohistochemistry; IF: immunofluorescence; LCM: laser capture microdissection; μCT: micro-computed tomography; MIF: macrophage migration inhibitory factor; MMP: matrix metalloproteinase; PKG: protein kinase G (PKG); PVDF: polyvinylidene fluoride; RT-qPCR: reverse transcription quantitative polymerase chain reaction; SDS-PAGE: sodium dodecyl sulfate polyacrylamide gel electrophoresis; shRNA: short hairpin RNA; TRAP: tartrate resistant acid phosphatase.

Competing interests

The authors declare that they have no competing interests.

Authors' contributions

AAM carried out the LCM, expression analysis and experiments focused on ABCC5 function. EA and MC collected the bone trephine biopsies from breast cancer patients with known bone involvement. ZD performed immunohistochemistry and immunofluorescence staining. KT and SVK conducted the *in vitro* osteoclastogenesis experiments. SC and MH conducted the gene expression analysis. AO identified regions of primary tumours and bone metastases suitable for LCM and scored the ABCC5 IHC staining. NB and MP generously provided primary breast tumour material. VO assisted in intra-cardiac injection of mammary tumour cells. GLS generously provided ABCC5 antibody. AAM and PMS designed the experiments, interpreted the results and prepared the manuscript. All authors read and approved the final manuscript.

Acknowledgements

This work was funded by grants from the CIHR (CIHR CTP-79857) and Genome Quebec. AAM was supported by a studentship from the FRSQ, VO by a fellowship from the CIHR and PMS received support as a Research Scholar (Junior II) of the FRSQ. We thank Dr. Ursini-Siegel and members of the Siegel laboratory for helpful discussions and their critical comments on the manuscript. We acknowledge infrastructure support and technical assistance for the LCM experiments from the Breast Cancer Functional Genomics Group (McGill University), which is supported by funds from the Terry Fox Foundation. The primary breast material collection was supported by the Database and Tissue Bank Axis of the Réseau de recherche en cancer of the Fonds de recherche du Québec - Santé (FRQS). The routine histology was provided by the Centre for Bone and

Periodontal Research (McGill University) and the Goodman Cancer Research Centre (McGill University). A.A.M. acknowledges studentship support from FRQS. P.M.S. acknowledges previous support as a Research Scholar (Junior II) of the FRQS. This work was supported by a team grant from the Canadian Institutes of Health Research (CIHR CTP-79857) and a CIHR operating grant to P.M.S. (MOP-119401).

References

1. Weilbaecher KN, Guise TA, McCauley LK: **Cancer to bone: a fatal attraction**. *Nat Rev Cancer* 2011, **11**:411-425.

2. Suva LJ, Washam C, Nicholas RW, Griffin RJ: **Bone metastasis: mechanisms and therapeutic opportunities**. *Nat Rev Endocrinol* 2011, **7**:208-218.

3. Kozlow W, Guise TA: **Breast cancer metastasis to bone: mechanisms of osteolysis and implications for therapy**. *J Mammary Gland Biol Neoplasia* 2005, **10**:169-180.

4. Rose AA, Siegel PM: **Breast cancer-derived factors facilitate osteolytic bone metastasis**. *Bull Cancer* 2006, **93**:931-943.

5. Yoneda T, Hiraga T: **Crosstalk between cancer cells and bone microenvironment in bone metastasis**. *Biochem Biophys Res Commun* 2005, **328**:679-687.

6. Casimiro S, Guise TA, Chirgwin J: **The critical role of the bone microenvironment in cancer metastases**. *Mol Cell Endocrinol* 2009, **310**:71-81.

7. Chen YC, Sosnoski DM, Mastro AM: **Breast cancer metastasis to the bone: mechanisms of bone loss**. *Breast Cancer Res* 2010, **12**:215.

8. Smid M, Wang Y, Klijn JG, Sieuwerts AM, Zhang Y, Atkins D, Martens JW, Foekens JA: **Genes associated with breast cancer metastatic to bone**. *J Clin Oncol* 2006, **24**:2261-2267.

9. Zhang XH, Wang Q, Gerald W, Hudis CA, Norton L, Smid M, Foekens JA, Massague J: **Latent bone metastasis in breast cancer tied to Src-dependent survival signals**. *Cancer Cell* 2009, **16**:67-78.

10. Kang Y, Siegel PM, Shu W, Drobnjak M, Kakonen SM, Cordon-Cardo C, Guise TA, Massague J: **A multigenic program mediating breast cancer metastasis to bone**. *Cancer Cell* 2003, **3**:537-549.

11. Ouellet V, Tiedemann K, Mourskaia A, Fong JE, Tran-Thanh D, Amir E, Clemons M, Perbal B, Komarova SV, Siegel PM: **CCN3 impairs osteoblast and stimulates osteoclast differentiation to favor breast cancer metastasis to bone**. *Am J Pathol* 2011, **178**:2377-2388.

12. Rose AA, Pepin F, Russo C, Abou Khalil JE, Hallett M, Siegel PM: **Osteoactivin promotes breast cancer metastasis to bone**. *Mol Cancer Res* 2007, **5**:1001-1014.

13. Yoneda T, Williams PJ, Hiraga T, Niewolna M, Nishimura R: **A bone-seeking clone exhibits different biological properties from the MDA-MB-231 parental human breast cancer cells and a brain-seeking clone in vivo and in vitro**. *J Bone Miner Res* 2001, **16**:1486-1495.

14. Arslan C, Sari E, Aksoy S, Altundag K: **Variation in hormone receptor and HER-2 status between primary and metastatic breast cancer: review of the literature**. *Expert Opin Ther Targets* 2011, **15**:21-30.

15. St Romain P, Madan R, Tawfik OW, Damjanov I, Fan F: **Organotropism and prognostic marker discordance in distant metastases of breast carcinoma: fact or fiction? A clinicopathologic analysis**. *Hum Pathol* 2012, **43**:398-404.

16. Amir E, Miller N, Geddie W, Freedman O, Kassam F, Simmons C, Oldfield M, Dranitsaris G, Tomlinson G, Laupacis A, Tannock IF, Clemons M: **Prospective study evaluating the impact of tissue confirmation of metastatic disease in patients with breast cancer**. *J Clin Oncol* 2012, **30**:587-592.

17. Hilton JF, Amir E, Hopkins S, Nabavi M, DiPrimio G, Sheikh A, Done SJ, Gianfelice D, Kanji F, Dent S, Barth D, Bouganim N, Al-Najjar A, Clemons M: **Acquisition of metastatic tissue from patients with bone metastases from breast cancer**. *Breast cancer research and treatment* 2011, **129**:761-765.

18. Gentleman RC, Carey VJ, Bates DM, Bolstad B, Dettling M, Dudoit S, Ellis B, Gautier L, Ge Y, Gentry J, Hornik K, Hothorn T, Huber W, Iacus S, Irizarry R, Leisch F, Li C, Maechler M, Rossini AJ, Sawitzki G, Smith C, Smyth G, Tierney

L, Yang JY, Zhang J: **Bioconductor: open software development for computational biology and bioinformatics**. *Genome Biol* 2004, **5**:R80.

19. **The National Center for Biotechnology Information** [http://www.ncbi.nlm.nih.gov/geo/query/acc.cgi?token=njwzhwsagooekps&acc=GSE39494]

20. Siegel PM, Ryan ED, Cardiff RD, Muller WJ: **Elevated expression of activated forms of Neu/ErbB-2 and ErbB-3 are involved in the induction of mammary tumors in transgenic mice: implications for human breast cancer**. *EMBO J* 1999, **18**:2149-2164.

21. **RNAi central** [http://katahdin.cshl.org/siRNA/RNAi.cgi?type=shRNA]

22. Dickins RA, Hemann MT, Zilfou JT, Simpson DR, Ibarra I, Hannon GJ, Lowe SW: **Probing tumor phenotypes using stable and regulated synthetic microRNA precursors**. *Nat Genet* 2005, **37**:1289-1295.

23. Minn AJ, Kang Y, Serganova I, Gupta GP, Giri DD, Doubrovin M, Ponomarev V, Gerald WL, Blasberg R, Massague J: **Distinct organ-specific metastatic potential of individual breast cancer cells and primary tumors**. *J Clin Invest* 2005, **115**:44-55.

24. Gupta GP, Minn AJ, Kang Y, Siegel PM, Serganova I, Cordon-Cardo C, Olshen AB, Gerald WL, Massague J: **Identifying site-specific metastasis genes and functions**. *Cold Spring Harb Symp Quant Biol* 2005, **70**:149-158.

25. Aslakson CJ, Miller FR: **Selective events in the metastatic process defined by analysis of the sequential dissemination of subpopulations of a mouse mammary tumor**. *Cancer research* 1992, **52**:1399-1405.

26. Armstrong S, Pereverzev A, Dixon SJ, Sims SM: **Activation of P2X7 receptors causes isoform-specific translocation of protein kinase C in osteoclasts**. *Journal of cell science* 2009, **122**:136-144.

27. Mourskaia AA, Dong Z, Ng S, Banville M, Zwaagstra JC, O'Connor-McCourt MD, Siegel PM: **Transforming growth factor-beta1 is the predominant isoform required for breast cancer cell outgrowth in bone**. *Oncogene* 2009, **28**:1005-1015.

28. Labelle-Cote M, Dusseault J, Ismail S, Picard-Cloutier A, Siegel PM, Larose L: **Nck2 promotes human melanoma cell proliferation, migration and invasion in vitro and primary melanoma-derived tumor growth in vivo**. *BMC Cancer* 2011, **11**:443.

29. Xu AJ, Xia XH, Du ST, Gu JC: **Clinical significance of PHPT1 protein expression in lung cancer**. *Chin Med J (Engl)* 2010, **123**:3247-3251.

30. McConnell BV, Koto K, Gutierrez-Hartmann A: **Nuclear and cytoplasmic LIMK1 enhances human breast cancer progression**. *Mol Cancer* 2011, **10**:75.

31. LaLonde DP, Brown MC, Bouverat BP, Turner CE: **Actopaxin interacts with TESK1 to regulate cell spreading on fibronectin**. *J Biol Chem* 2005, **280**:21680-21688.

32. Liu CR, Ma CS, Ning JY, You JF, Liao SL, Zheng J: **Differential thymosin beta 10 expression levels and actin filament organization in tumor cell lines with different metastatic potential**. *Chin Med J (Engl)* 2004, **117**:213-218.

33. Mochizuki S, Okada Y: **ADAMs in cancer cell proliferation and progression**. *Cancer Sci* 2007, **98**:621-628.

34. Mannello F: **What does matrix metalloproteinase-1 expression in patients with breast cancer really tell us?** *BMC Med* 2011, **9**:95.

35. Steenport M, Khan KM, Du B, Barnhard SE, Dannenberg AJ, Falcone DJ: **Matrix metalloproteinase (MMP)-1 and MMP-3 induce macrophage MMP-9: evidence for the role of TNF-alpha and cyclooxygenase-2**. *J Immunol* 2009, **183**:8119-8127.

36. Albig AR, Becenti DJ, Roy TG, Schiemann WP: **Microfibril-associate glycoprotein-2 (MAGP-2) promotes angiogenic cell sprouting by blocking notch signaling in endothelial cells**. *Microvasc Res* 2008, **76**:7-14.

37. Courtwright A, Siamakpour-Reihani S, Arbiser JL, Banet N, Hilliard E, Fried L, Livasy C, Ketelsen D, Nepal DB, Perou CM, Patterson C, Klauber-Demore N: **Secreted frizzle-related protein 2 stimulates angiogenesis via a calcineurin/NFAT signaling pathway**. *Cancer research* 2009, **69**:4621-4628.

38. Amin EM, Oltean S, Hua J, Gammons MV, Hamdollah-Zadeh M, Welsh GI, Cheung MK, Ni L, Kase S, Rennel ES, Symonds KE, Nowak DG, Royer-Pokora B, Saleem MA, Hagiwara M, Schumacher VA, Harper SJ, Hinton DR, Bates DO,

Ladomery MR: **WT1 mutants reveal SRPK1 to be a downstream angiogenesis target by altering VEGF splicing**. *Cancer Cell* 2011, **20**:768-780.

39. McMahon G: **VEGF receptor signaling in tumor angiogenesis**. *Oncologist* 2000, **5 Suppl 1**:3-10.

40. Shao R, Hamel K, Petersen L, Cao QJ, Arenas RB, Bigelow C, Bentley B, Yan W: **YKL-40, a secreted glycoprotein, promotes tumor angiogenesis**. *Oncogene* 2009, **28**:4456-4468.

41. Chan AS, Jensen KK, Skokos D, Doty S, Lederman HK, Kaplan RN, Rafii S, Rivella S, Lyden D: **Id1 represses osteoclast-dependent transcription and affects bone formation and hematopoiesis**. *PLoS One* 2009, **4**:e7955.

42. Nakayama S, Iida K, Tsuzuki T, Iwashita T, Murakami H, Asai N, Iwata Y, Ichihara M, Ito S, Kawai K, Asai M, Kurokawa K, Takahashi M: **Implication of expression of GDNF/Ret signalling components in differentiation of bone marrow haemopoietic cells**. *Br J Haematol* 1999, **105**:50-57.

43. Suh HC, Ji M, Gooya J, Lee M, Klarmann KD, Keller JR: **Cell-nonautonomous function of Id1 in the hematopoietic progenitor cell niche**. *Blood* 2009, **114**:1186-1195.

44. Ding XW, Wu JH, Jiang CP: **ABCG2: a potential marker of stem cells and novel target in stem cell and cancer therapy**. *Life sciences* 2010, **86**:631-637.

45. Kaplan RN, Psaila B, Lyden D: **Bone marrow cells in the 'pre-metastatic niche': within bone and beyond**. *Cancer Metastasis Rev* 2006, **25**:521-529.

46. Shiozawa Y, Pedersen EA, Havens AM, Jung Y, Mishra A, Joseph J, Kim JK, Patel LR, Ying C, Ziegler AM, Pienta MJ, Song J, Wang J, Loberg RD, Krebsbach PH, Pienta KJ, Taichman RS: **Human prostate cancer metastases target the hematopoietic stem cell niche to establish footholds in mouse bone marrow**. *J Clin Invest* 2011, **121**:1298-1312.

47. Kelly PN, Strasser A: **The role of Bcl-2 and its pro-survival relatives in tumourigenesis and cancer therapy**. *Cell Death Differ* 2011, **18**:1414-1424.

48. Kutuzov MA, Bennett N, Andreeva AV: **Protein phosphatase with EF-hand domains 2 (PPEF2) is a potent negative regulator of apoptosis signal regulating kinase-1 (ASK1)**. *Int J Biochem Cell Biol* 2010, **42**:1816-1822.

49. Kaufmann T, Strasser A, Jost PJ: **Fas death receptor signalling: roles of Bid and XIAP**. *Cell Death Differ* 2012, **19**:42-50.

50. Szigeti A, Bellyei S, Gasz B, Boronkai A, Hocsak E, Minik O, Bognar Z, Varbiro G, Sumegi B, Gallyas F, Jr.: **Induction of necrotic cell death and mitochondrial permeabilization by heme binding protein 2/SOUL**. *FEBS Lett* 2006, **580**:6447-6454.

51. Micali N, Ferrai C, Fernandez-Diaz LC, Blasi F, Crippa MP: **Prep1 directly regulates the intrinsic apoptotic pathway by controlling Bcl-XL levels**. *Molecular and cellular biology* 2009, **29**:1143-1151.

52. Schulz R, Marchenko ND, Holembowski L, Fingerle-Rowson G, Pesic M, Zender L, Dobbelstein M, Moll UM: **Inhibiting the HSP90 chaperone destabilizes macrophage migration inhibitory factor and thereby inhibits breast tumor progression**. *J Exp Med* 2012, **209**:275-289.

53. Lim S, Choong LY, Kuan CP, Yunhao C, Lim YP: **Regulation of macrophage inhibitory factor (MIF) by epidermal growth factor receptor (EGFR) in the MCF10AT model of breast cancer progression**. *J Proteome Res* 2009, **8**:4062-4076.

54. Xu X, Wang B, Ye C, Yao C, Lin Y, Huang X, Zhang Y, Wang S: **Overexpression of macrophage migration inhibitory factor induces angiogenesis in human breast cancer**. *Cancer Lett* 2008, **261**:147-157.

55. Lue H, Thiele M, Franz J, Dahl E, Speckgens S, Leng L, Fingerle-Rowson G, Bucala R, Luscher B, Bernhagen J: **Macrophage migration inhibitory factor (MIF) promotes cell survival by activation of the Akt pathway and role for CSN5/JAB1 in the control of autocrine MIF activity**. *Oncogene* 2007, **26**:5046-5059.

56. Bando H, Matsumoto G, Bando M, Muta M, Ogawa T, Funata N, Nishihira J, Koike M, Toi M: **Expression of macrophage migration inhibitory factor in human breast cancer: association with nodal spread**. *Jpn J Cancer Res* 2002, **93**:389-396.

57. Verjans E, Noetzel E, Bektas N, Schutz AK, Lue H, Lennartz B, Hartmann A, Dahl E, Bernhagen J: **Dual role of macrophage migration inhibitory factor (MIF) in human breast cancer**. *BMC Cancer* 2009, **9**:230.

58. Jacquin C, Koczon-Jaremko B, Aguila HL, Leng L, Bucala R, Kuchel GA, Lee SK: **Macrophage migration inhibitory factor inhibits osteoclastogenesis**. *Bone* 2009, **45**:640-649.

59. Natarajan K, Xie Y, Baer MR, Ross DD: **Role of breast cancer resistance protein (BCRP/ABCG2) in cancer drug resistance**. *Biochemical pharmacology* 2012, **83**:1084-1103.

60. **Human ABC-Transporters** [http://nutrigene.4t.com/humanabc.htm]

61. Vasiliou V, Vasiliou K, Nebert DW: **Human ATP-binding cassette (ABC) transporter family**. *Hum Genomics* 2009, **3**:281-290.

62. Farke C, Meyer HH, Bruckmaier RM, Albrecht C: **Differential expression of ABC transporters and their regulatory genes during lactation and dry period in bovine mammary tissue**. *J Dairy Res* 2008, **75**:406-414.

63. van Herwaarden AE, Wagenaar E, Merino G, Jonker JW, Rosing H, Beijnen JH, Schinkel AH: **Multidrug transporter ABCG2/breast cancer resistance protein secretes riboflavin (vitamin B2) into milk**. *Molecular and cellular biology* 2007, **27**:1247-1253.

64. Dean M: **ABC transporters, drug resistance, and cancer stem cells**. *J Mammary Gland Biol Neoplasia* 2009, **14**:3-9.

65. Jedlitschky G, Burchell B, Keppler D: **The multidrug resistance protein 5 functions as an ATP-dependent export pump for cyclic nucleotides**. *J Biol Chem* 2000, **275**:30069-30074.

66. Pratt S, Shepard RL, Kandasamy RA, Johnston PA, Perry W, 3rd, Dantzig AH: **The multidrug resistance protein 5 (ABCC5) confers resistance to 5-fluorouracil and transports its monophosphorylated metabolites**. *Molecular cancer therapeutics* 2005, **4**:855-863.

67. Park S, Shimizu C, Shimoyama T, Takeda M, Ando M, Kohno T, Katsumata N, Kang YK, Nishio K, Fujiwara Y: **Gene expression profiling of ATP-binding cassette (ABC) transporters as a predictor of the pathologic response to neoadjuvant chemotherapy in breast cancer patients**. *Breast cancer research and treatment* 2006, **99**:9-17.

68. Saravani R, Karami-Tehrani F, Hashemi M, Aghaei M, Edalat R: **Inhibition of phosphodiestrase 9 induces cGMP accumulation and apoptosis in human breast cancer cell lines, MCF-7 and MDA-MB-468**. *Cell Prolif* 2012, **45**:199-206.

69. Fallahian F, Karami-Tehrani F, Salami S, Aghaei M: **Cyclic GMP induced apoptosis via protein kinase G in oestrogen receptor-positive and -negative breast cancer cell lines**. *FEBS J* 2011, **278**:3360-3369.

70. Mujoo K, Sharin VG, Martin E, Choi BK, Sloan C, Nikonoff LE, Kots AY, Murad F: **Role of soluble guanylyl cyclase-cyclic GMP signaling in tumor cell proliferation**. *Nitric Oxide* 2010, **22**:43-50.

71. Teixeira CC, Agoston H, Beier F: **Nitric oxide, C-type natriuretic peptide and cGMP as regulators of endochondral ossification**. *Developmental biology* 2008, **319**:171-178.

72. Babykutty S, Suboj P, Srinivas P, Nair AS, Chandramohan K, Gopala S: **Insidious role of nitric oxide in migration/invasion of colon cancer cells by upregulating MMP-2/9 via activation of cGMP-PKG-ERK signaling pathways**. *Clinical & experimental metastasis* 2012, **29**:471-492.

73. Ridnour LA, Windhausen AN, Isenberg JS, Yeung N, Thomas DD, Vitek MP, Roberts DD, Wink DA: **Nitric oxide regulates matrix metalloproteinase-9 activity by guanylyl-cyclase-dependent and -independent pathways**. *Proceedings of the National Academy of Sciences of the United States of America* 2007, **104**:16898-16903.

74. Akool el S, Kleinert H, Hamada FM, Abdelwahab MH, Forstermann U, Pfeilschifter J, Eberhardt W: **Nitric oxide increases the decay of matrix metalloproteinase 9 mRNA by inhibiting the expression of mRNA-stabilizing factor HuR**. *Molecular and cellular biology* 2003, **23**:4901-4916.

75. Lubbe WJ, Zuzga DS, Zhou Z, Fu W, Pelta-Heller J, Muschel RJ, Waldman SA, Pitari GM: **Guanylyl cyclase C prevents colon cancer metastasis by regulating**

tumor epithelial cell matrix metalloproteinase-9. *Cancer research* 2009, **69**:3529-3536.

76. Dong SS, Williams JP, Jordan SE, Cornwell T, Blair HC: **Nitric oxide regulation of cGMP production in osteoclasts**. *Journal of cellular biochemistry* 1999, **73**:478-487.

77. Yaroslavskiy BB, Li Y, Ferguson DJ, Kalla SE, Oakley JI, Blair HC: **Autocrine and paracrine nitric oxide regulate attachment of human osteoclasts**. *Journal of cellular biochemistry* 2004, **91**:962-972.

78. Yaroslavskiy BB, Zhang Y, Kalla SE, Garcia Palacios V, Sharrow AC, Li Y, Zaidi M, Wu C, Blair HC: **NO-dependent osteoclast motility: reliance on cGMP-dependent protein kinase I and VASP**. *Journal of cell science* 2005, **118**:5479-5487.

Figure 1. Laser capture microdissection (LCM) of breast cancer cells. Malignant mammary epithelial cells were isolated from primary breast tumours (top panels) and bone trephines (bottom panels). The selected regions containing the breast cancer cells were adhered to LCM caps (right panels). Left panels represent images of slides following completion of LCM with black arrows indicating the isolated material. The scale bar on the top left image represents 1000μm and applies to all panels.

Figure 2. ABCC5 expression is elevated in breast cancer bone metastases. A, *ABCC5* gene expression was found to be significantly overexpressed in breast cancer bone metastases (BM) compared to primary breast tumours (BT) that were metastatic to bone by both Agilent microarray analysis (*left panel*) and RT-qPCR (*right panel*). (*, P = 0.002, **, P = 0.03) B, Immunohistochemical (IHC) analysis confirmed that ABCC5 expression was higher in bone metastases (*right panels*) compared to primary breast tumours (*left panels*). IHC was performed on frozen sections for all the samples and the ABCC5 staining intensity is indicated in the lower left corner of each image. Scale bar in the first panel represents 100 μm and applies to all images.

Figure 3. ABCC5 promotes the formation of osteolytic bone metastases in MDA-MB-231 human breast cancer cells. A, ABCC5 expression is appreciably higher in the bone metastatic 1833-BM1 population compared to parental MDA-MB-231 cells and the lung metastatic 4175-LM2 population. B, Immunoblot analysis reveals that ABCC5 expression was efficiently silenced via short hairpin RNA (shRNA) in the 1833-BM1 breast cancer cell line. An immunoblot for α-Tubulin served as a loading control in panels (A) and (B). C, Diminished ABCC5 expression in 1833-BM1 cells resulted in reduced formation of skeletal metastases following cardiac injection as determined by *in vivo* bioluminescent imaging. The data and representative images are shown for day 21-post tumour cell injection (scr shRNA, n = 10; *ABCC5* shRNA, n = 8; *, P = 0.024). D, All of the animals developed osteolytic lesions following injection of the breast cancer cells. The number of lesions per animal was determined by analyzing blinded μCT images. E, The degree of osteolytic bone destruction was quantified by *in vivo* μCT imaging. Bone volume was calculated from reconstructions of defined regions of both the

proximal tibia and femur from mice imaged on day 21-post injection (scr shRNA, n = 20; *ABCC5* shRNA, n = 16; **, $P = 0.041$). Controls (n = 10) refers to age-matched females mice that were not injected with breast cancer cells. Representative images of bone reconstructions are shown.

Figure 4. ABCC5 promotes the formation of osteolytic bone metastases induced by 4T1 murine breast cancer cells. A, ABCC5 expression is considerably elevated in the highly metastatic mouse breast cancer cell line 4T1, which exhibits bone metastatic activity, when compared to a less metastatic 66cl4 (lung) and non-metastatic 67NR populations. B, ABCC5 expression was stably silenced using two independent short hairpin RNAs (sh#1, sh#2) in 4T1 breast cancer cells, as demonstrated by immunoblot analysis, when compared to parental 4T1 cells (4T1p) and a scrambled shRNA control (Scr shRNA). C, All of the animals presented with osteolytic lesions following breast cancer cell injections. The number of lesions per animal is indicated and was established by examining blinded μCT images. D, Reduction in ABCC5 levels in 4T1 breast cancer cells results in the diminished formation of osteolytic bone metastases following cardiac injection (scr shRNA, n = 19; *abcc5* shRNA #1, n = 16; *abcc5* shRNA #2, n = 19; *, $P = 0.015$; **, $P < 0.001$). Controls (n = 18) refers to age-matched female mice that were not injected with breast cancer cells. The degree of osteolytic bone destruction in the hindlimbs was quantified by *in vivo* μCT imaging. Bone volume of defined regions of both the proximal tibia and femur shown for animals imaged on day 21-post injection. Representative images of bone reconstructions are shown.

Figure 5. Loss of ABCC5 in breast cancer cells results in diminished osteoclast numbers within osteolytic lesions. A, Quantification of TRAP positive osteoclasts

within osteolytic lesions formed by human-derived 1833-BM1 cells (scr shRNA, n = 7; *ABCC5* shRNA, n = 7; *, $P = 0.03$). Representative images are shown for each group. The scale bars represent 100μm and applies to both images. B, Quantification of TRAP-positive cells present within bone metastases formed in mice injected with 4T1-derived populations (scr shRNA, n = 8; *abcc5* shRNA #1, n = 6; *abcc5* shRNA #2, n = 5; **, $P < 0.001$; ***, $P < 0.001$). Representative images are shown for each group. The scale bar in the upper image represents 100μm and applies to all images.

Figure 6. Loss of ABCC5 in breast cancer cells results in diminished osteoclast differentiation *in vitro*. Mouse bone marrow cells were primed with M-CSF and RANKL for 3 days and then cultured for 2 days untreated (negative control, NC), RANKL treated (positive control, PC), or conditioned media from 4T1-derived populations (scrambled shRNA (Scr), abcc5 shRNA #1 and abcc5 shRNA #2). Osteoclasts were counted for each condition and the results expressed as a percentage of the osteoclast number in the positive control. The data is presented as averages of 5 independent experiments (*, $P < 0.05$). Representative images are presented for each group. The scale bar in the first image represents 100μm and applies to all images.

Additional files

Additional file 1

Title: Supplemental Materials and Methods.

Description: This file contains the experimental procedures not presented in the main text.

Additional file 2

Title: Supplemental Table 1- Clinical data of the breast cancer samples.

Description: This table describes the clinical data of the breast cancer samples used in the study.

Additional file 3

Title: Figure S1 - Histological appearance of primary breast tumours and breast cancer bone metastases.

Description: All of the samples used for the study were reviewed by a breast pathologist. Bone metastases samples primarily consist of the malignant mammary epithelium and stroma. The primary tumour material displays more complexity. All of the primary breast

tumour samples contained invasive epithelia cells and stroma. In addition, some of the samples included ductal carcinoma *in situ* (DCIS) as well as normal and hyperplastic mammary ducts. Scale bar represents 50 μm and applies to all the images.

Additional file 4

Title: Figure S2 - Human breast cancer metastases express basal keratins or co-express basal and luminal keratins.

Description: The expression of cytokeratin 8/18 (CK8/18) and cytokeratin 5 (CK5) in breast cancer bone metastases was assessed via immunofluorescence. All of the bone metastases stained positive for the myo-epithelial marker CK5, implying their basal-like phenotype. Three out of five bone metastases also stained positive for the luminal marker, CK8/18. The images were taken on a confocal microscope under the 63X objective. The scale bar represents 20μm and applies to all the images.

Additional file 5

Title: Microarray Data

Description: This is a list of differentially expressed probes between bone trephine biopsies from breast cancer patients and primary breast tumours metastatic to skeleton.

Additional file 6

Title: Figure S3 - Categories of genes that are differentially expressed in the breast cancer bone metastases compared to the primary breast tumours that were metastatic to bone.

Description: Application of filter criteria described in the materials and methods resulted in a list of 244 overexpressed and 185 underexpressed probes in breast cancer skeletal metastases compared to primary breast tumours. This list was further condensed to 118 up-regulated and 82 down-regulated genes when only unique genes with described functions were considered. These genes were subcategorized on the basis of their known functions.

Additional file 7

Title: Figure S4 - Agilent gene expression data of genes selected for RT-qPCR validation.

Description: A subset of candidate genes that were differentially expressed between breast cancer bone metastases and primary tumours are shown. Several members of the ATP-binding cassette (ABC) transporter family were found to be over-expressed in breast cancer bone metastases relative to the primary tumours metastatic to bone.

Additional file 8

Title: Figure S5 - RT-qPCR validation of genes that are differentially expressed between primary breast tumours and breast cancer bone metastases.

Description: The Agilent gene expression data were validated at the message level by RT-qPCR. A high degree of concordance between the Agilent microarray expression data (Additional File 7 - Figure S4) and the RT-qPCR analysis was observed.

Additional file 9

Title: Figure S6 - Reduced ABCC5 expression does not alter growth characteristics of MDA-MB-231 human or 4T1 mouse breast cancer cells.

Description: A, *In vitro* growth curves for 1833-BM1 cells expressing either scrambled (Scr shRNA) or *ABCC5* specific short hairpin RNAs (*ABCC5* shRNA) are shown. The average of three independent wells is presented for each time point. The error bars denote the standard error of the mean (SEM). B, Tumour growth curves following mammary fat pad injection are shown. Mammary tumour growth was measured biweekly for 29 days in mice injected with 1833-BM1 expressing Scr shRNA (n = 14) or *ABCC5* shRNAs (n = 16). Error bars signify the SEM for each time point. C, *In vitro* growth curves are shown for 4T1-derived breast cancer cells expressing either scrambled (Scr shRNA) or *ABCC5* specific short hairpin RNAs (*ABCC5* shRNA). The average of three independent wells is presented for each time point. The error bars denote the standard error of the mean (SEM). D, Growth of 4T1-derived mammary tumours in syngeneic mice following mammary fat pad injection is shown. Mammary tumour growth was measured biweekly for 36 days in mice injected with 4T1 cells expressing Scr shRNAs (n = 10) or two independent *ABCC5* shRNAs [shRNA1 (n = 10) or shRNA2 (n = 10)]. Error bars signify the SEM for each time point.

Additional file 10

Title: Figure S7 - Reduced ABCC5 expression does not alter spontaneous lung metastasis burden in mice bearing 4T1-derived mammary tumours.

Description: Lungs from mice bearing 4T1 tumours expressing Scr shRNA (n = 5) or two independent *ABCC5* shRNAs [shRNA1 (n = 5) or shRNA2 (n = 5)] extracted at end point and were stained with H&E. The number of lesions per lung (A) and the total lesion area per lung (B) were analysed. The error bars represent the standard error of the mean and apply to all the graphs.

Additional file 11

Title: Figure S8 - Reduced ABCC5 expression does not alter the proliferative index of human MDA-MB-231 or mouse 4T1 primary tumours nor bone metastases at end stage.

Description: A, Primary tumours derived from mice injected with 1833-BM1 cells expressing Scr shRNA (n = 5) or *ABCC5* shRNA (n = 5) on day 29 post injection were stained against Ki67. B, Primary tumours derived from mice injected with 4T1 cells expressing Scr shRNAs (n = 5) or two independent *ABCC5* shRNAs [shRNA1 (n = 5) or shRNA2 (n = 5)] on day 36 post injection were stained against Ki67. C, Hindlimbs with bone metastases formed from the intracardiac injection of 1833-BM1 cells expressing Scr shRNA (n = 5) or *ABCC5* shRNA (n = 5) on day 21 post inoculation were stained against

Ki67. D, Hindlims with bone metastases formed from the intracardiac injection of 4T1 cells expressing Scr shRNAs (n = 5) or two independent *ABCC5* shRNAs [shRNA1 (n = 5) or shRNA2 (n = 5)] on day 13 post inoculation were stained against Ki67. Proliferation is expressed as the percentage of Ki67-positive nuclei. The error bars represent the standard error of the mean and apply to all the graphs.

Additional file 12

Title: Figure S9 - Reduced ABCC5 expression does not alter the apoptosis of human MDA-MB-231 or mouse 4T1 primary tumours nor bone metastases at end stage.

Description: A, Primary tumours derived from mice injected with 1833-BM1 cells expressing Scr shRNA (n = 5) or *ABCC5* shRNA (n = 5) on day 29 post injection were stained against cleaved caspase-3. B, Primary tumours derived from mice injected with 4T1 cells expressing Scr shRNAs (n = 5) or two independent *ABCC5* shRNAs [shRNA1 (n = 5) or shRNA2 (n = 5)] on day 36 post injection were stained against cleaved caspase-3. C, Hindlims with bone metastases formed from the intracardiac injection of 1833-BM1 cells expressing Scr shRNA (n = 5) or *ABCC5* shRNA (n = 5) on day 21 post inoculation were stained against cleaved caspase-3. D, Hindlims with bone metastases formed from the intracardiac injection of 4T1 cells expressing Scr shRNAs (n = 5) or two independent *ABCC5* shRNAs [shRNA1 (n = 5) or shRNA2 (n = 5)] on day 13 post inoculation were stained against cleaved caspase-3. Apoptosis is expressed as the number of cleaved caspase-3-positive nuclei per 1000 cells. The error bars represent the standard error of the mean and apply to all the graphs.

Breast Cancer Bone Metastases

Primary Breast Tumor

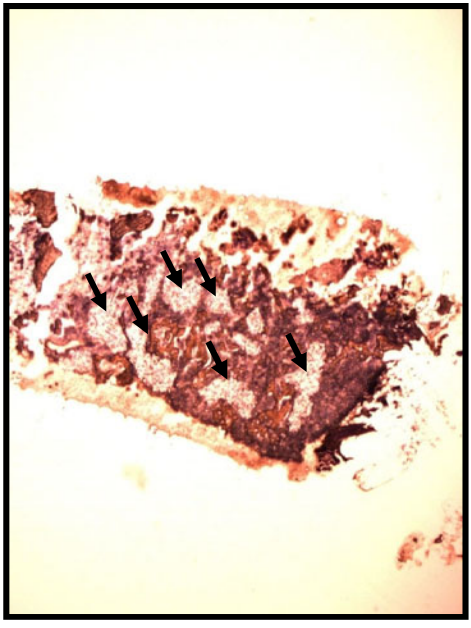

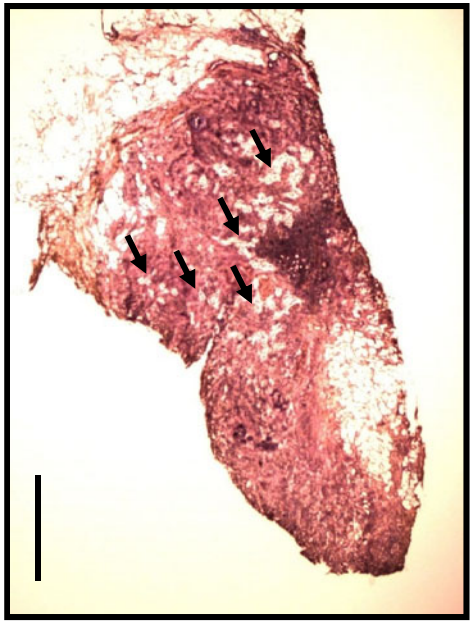

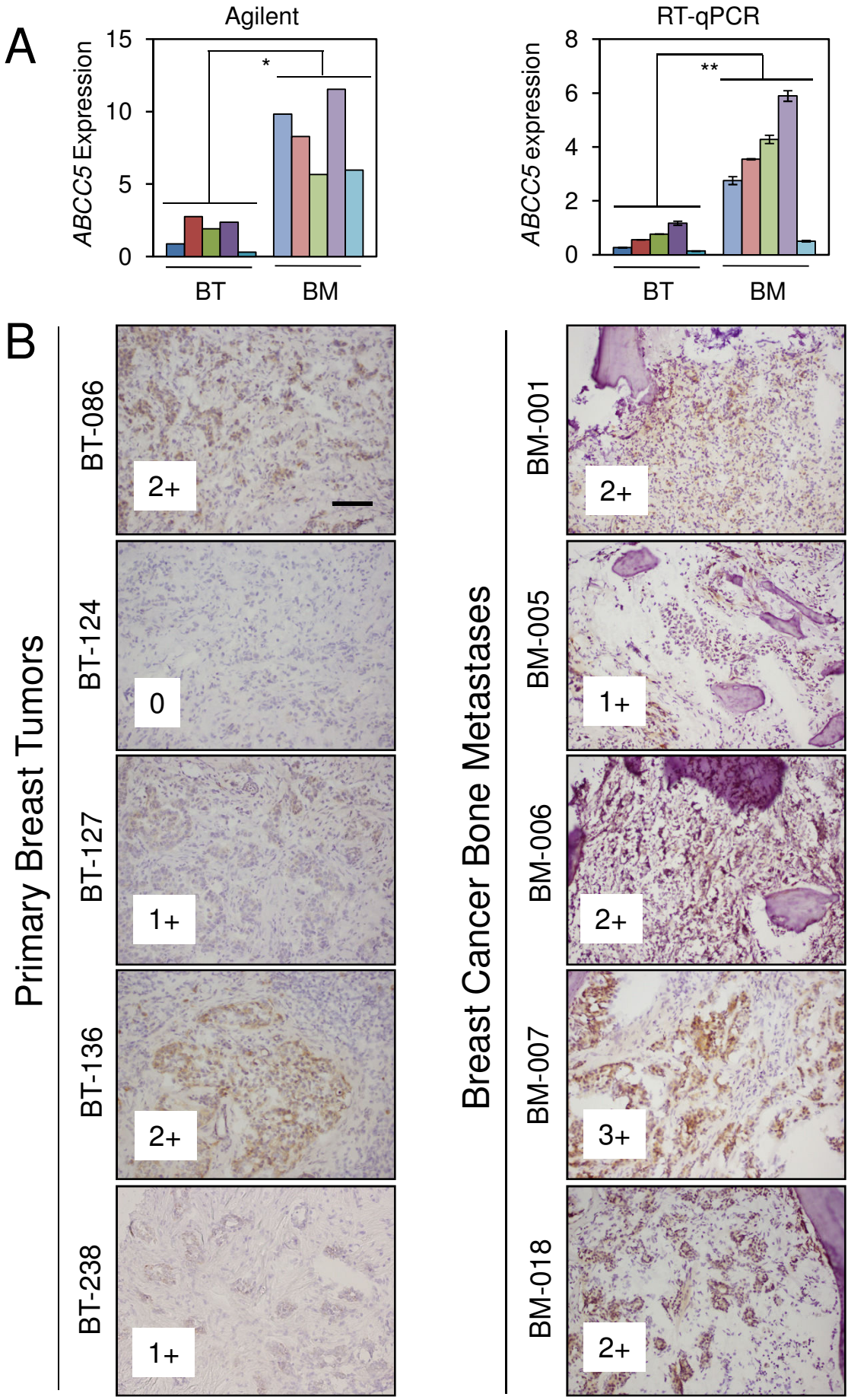
A
Agilent
ABCC5 Expression
15
10
5
0
*
BT
BM
RT-qPCR
ABCC5 expression
8
6
4
2
0
**
BT
BM
B
Primary Breast Tumors
BT-086
2+
BT-124
0
BT-127
1+
BT-136
2+
BT-238
1+
Breast Cancer Bone Metastases
BM-001
2+
BM-005
1+
BM-006
2+
BM-007
3+
BM-018
2+

Figure 3

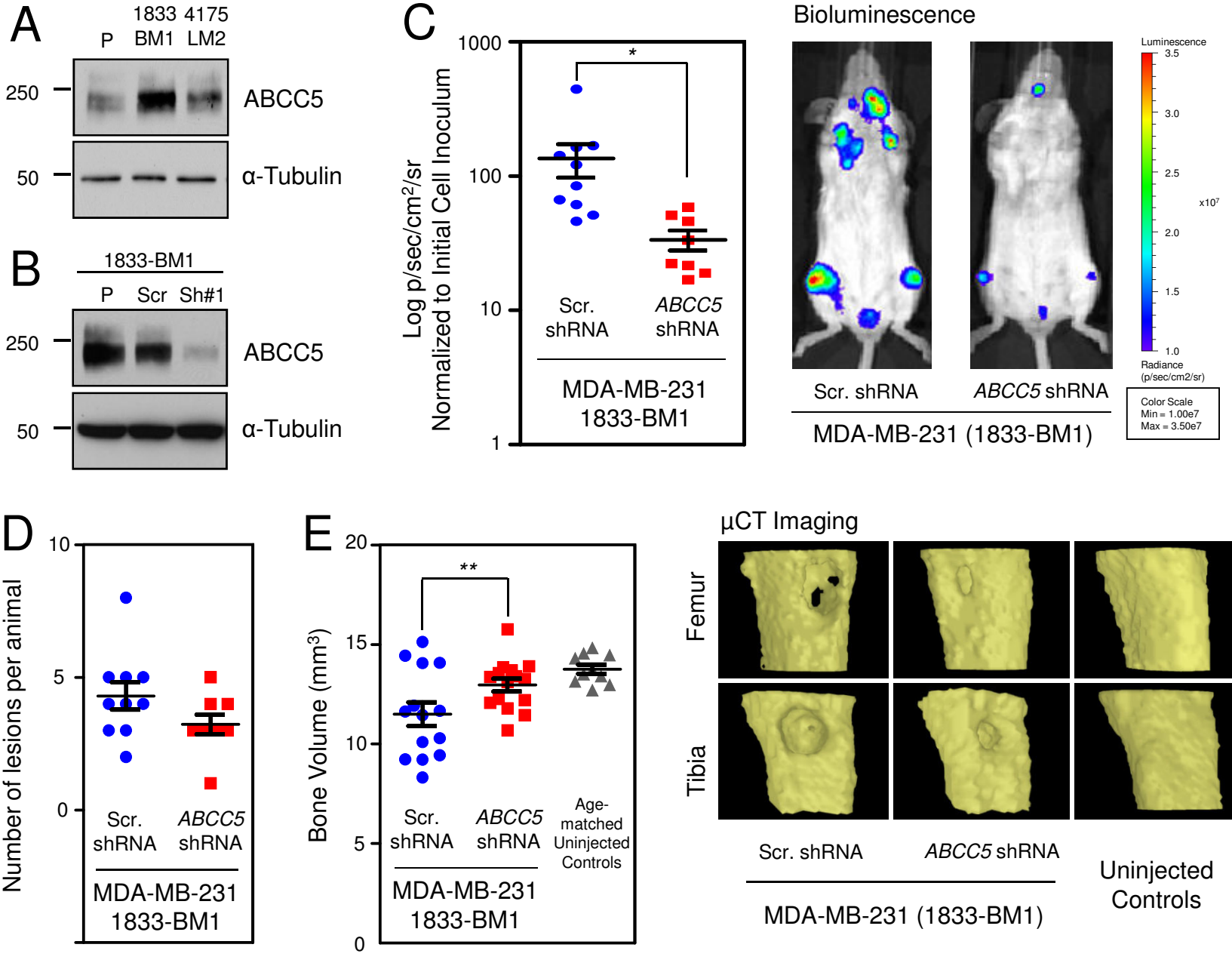
A
P
1833 BM1
4175 LM2
250
50
ABCC5
α-Tubulin
B
1833-BM1
P
Scr
Sh#1
250
50
ABCC5
α-Tubulin
C
Log p/sec/cm2/sr
Normalized to Initial Cell Inoculum
1000
100
10
1
*
Scr. shRNA
ABCC5 shRNA
MDA-MB-231
1833-BM1
Bioluminescence
Luminescence
3.5
3.0
2.5
x10^7
2.0
1.5
1.0
Radiance (p/sec/cm2/sr)
Color Scale
Min = 1.00e7
Max = 3.50e7
Scr. shRNA
ABCC5 shRNA
MDA-MB-231 (1833-BM1)
D
Number of lesions per animal
10
5
0
Scr. shRNA
ABCC5 shRNA
MDA-MB-231
1833-BM1
E
Bone Volume (mm3)
20
15
10
5
0
**
Scr. shRNA
ABCC5 shRNA
Age-matched Uninjected Controls
MDA-MB-231
1833-BM1
µCT Imaging
Femur
Tibia
Scr. shRNA
ABCC5 shRNA
Uninjected Controls
MDA-MB-231 (1833-BM1)

Figure 4

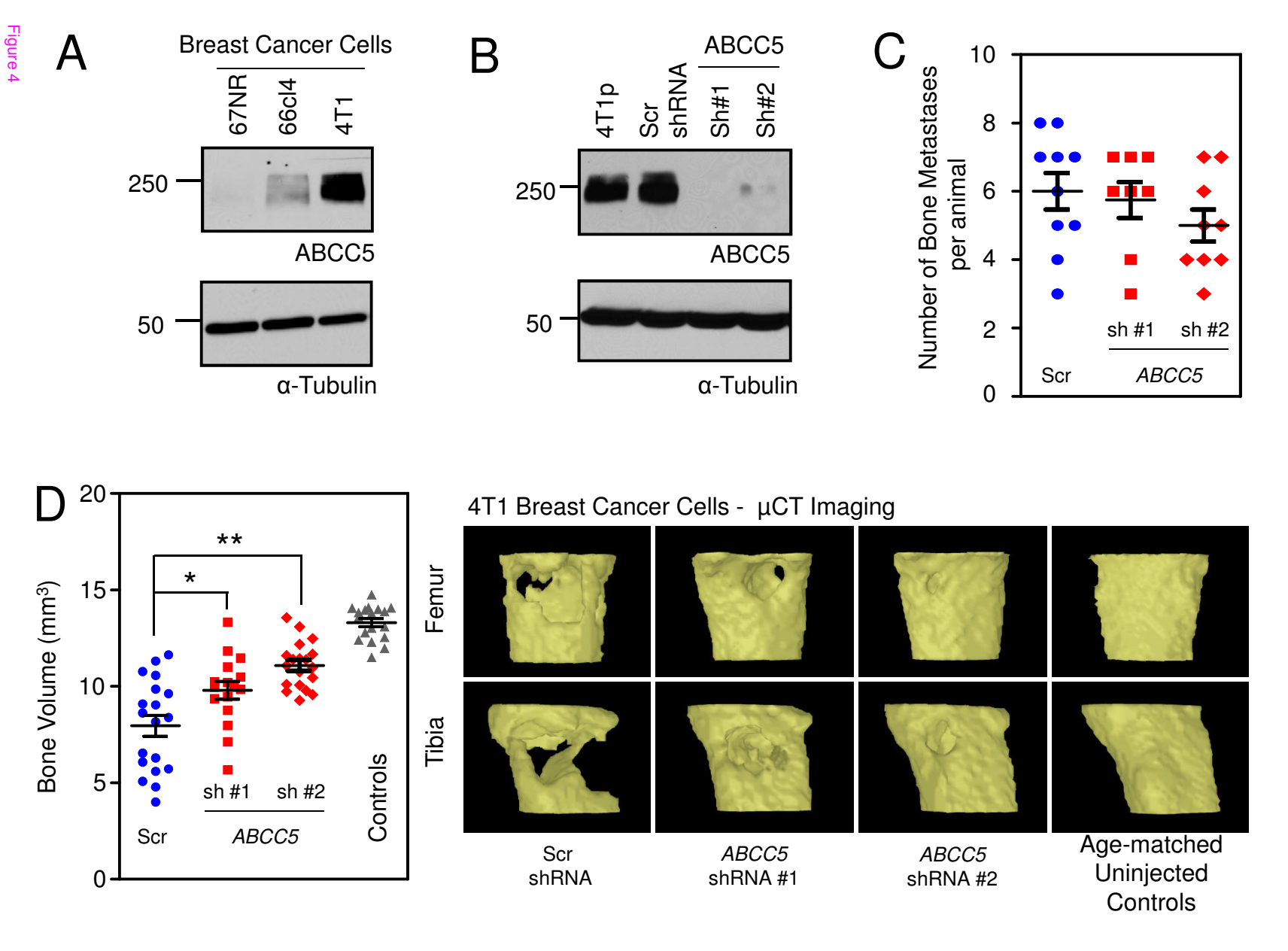
A
Breast Cancer Cells
67NR
66cl4
4T1
250
ABCC5
50
α-Tubulin
B
ABCC5
4T1p
Scr shRNA
Sh#1
Sh#2
250
ABCC5
50
α-Tubulin
C
Number of Bone Metastases per animal
10
8
6
4
2
0
sh #1
sh #2
Scr
ABCC5
D
Bone Volume (mm³)
20
15
10
5
0
**
*
sh #1
sh #2
Scr
ABCC5
Controls
4T1 Breast Cancer Cells - µCT Imaging
Femur
Tibia
Scr shRNA
ABCC5 shRNA #1
ABCC5 shRNA #2
Age-matched Uninjected Controls

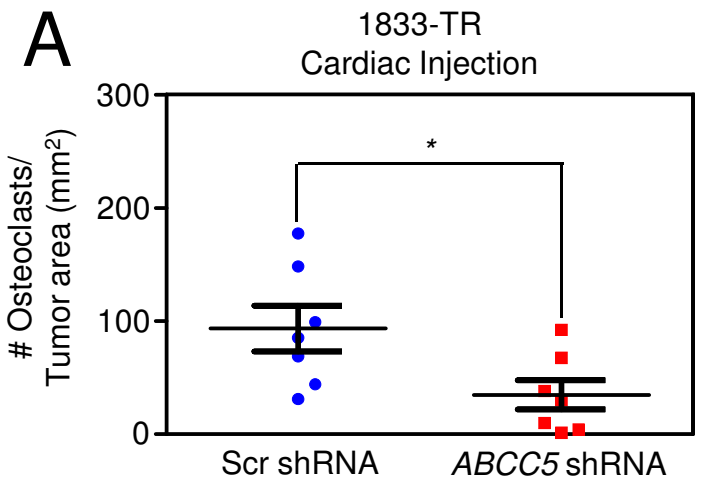

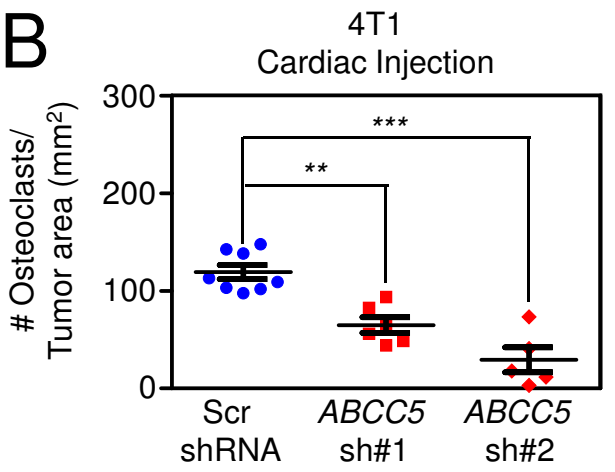

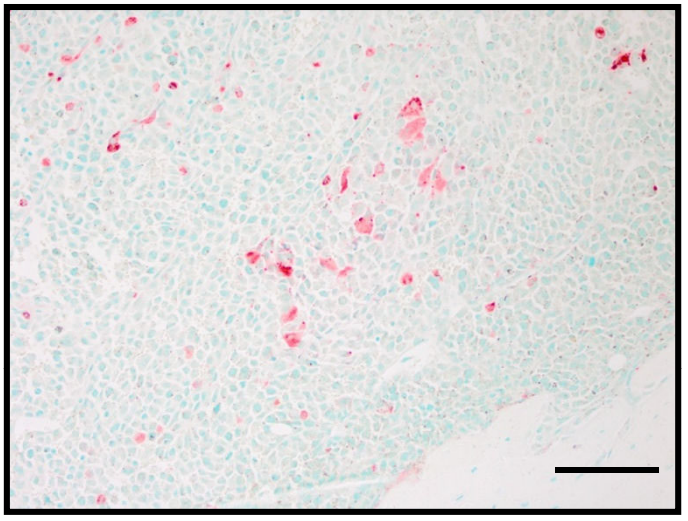

1833-TR Scr shRNA

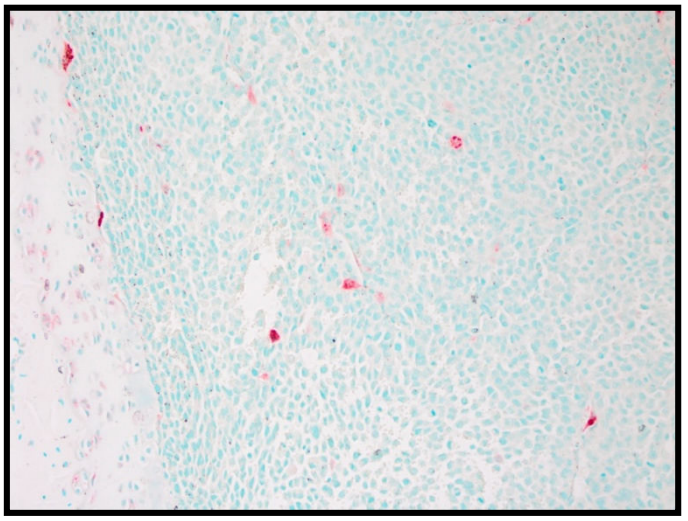

1833-TR *ABCC5* shRNA

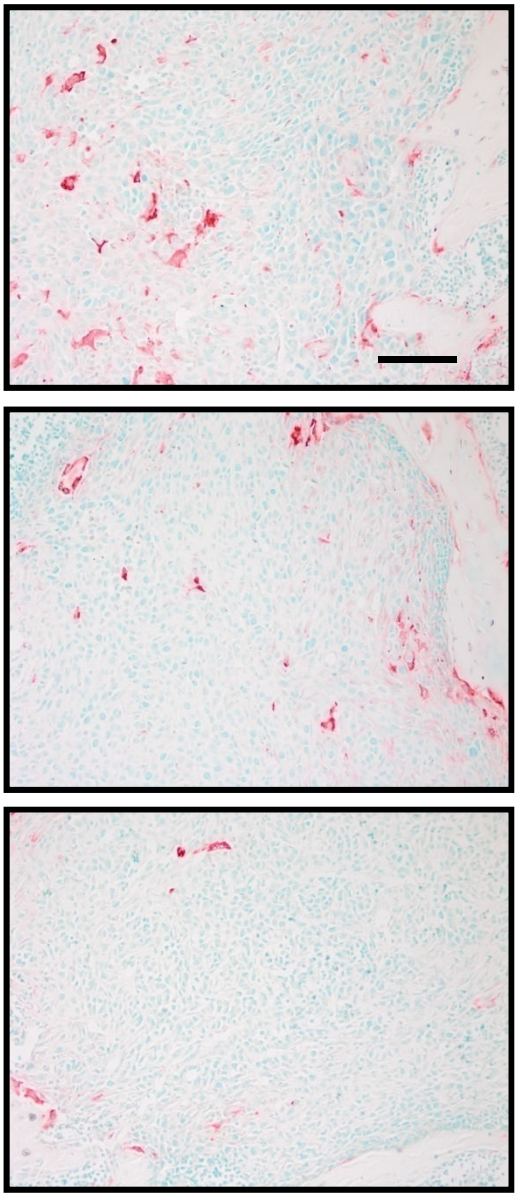

Figure 5

Figure 6

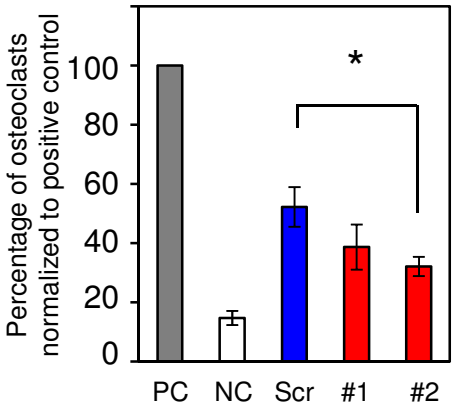

Positive Control (PC)

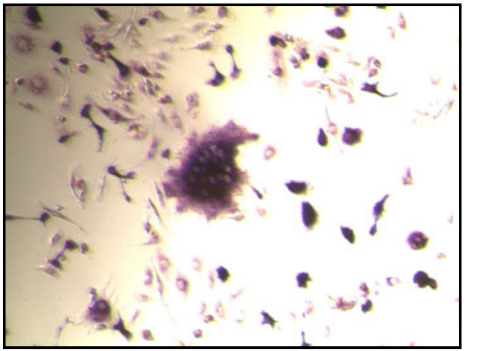

Negative Control (NC)

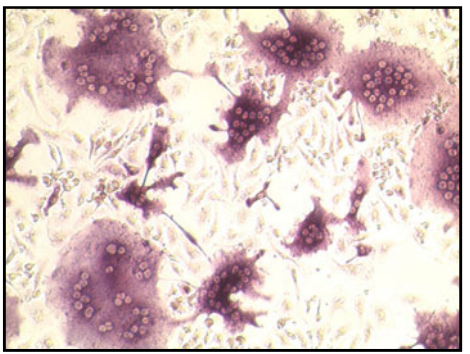

4T1 CM – Scr shRNA

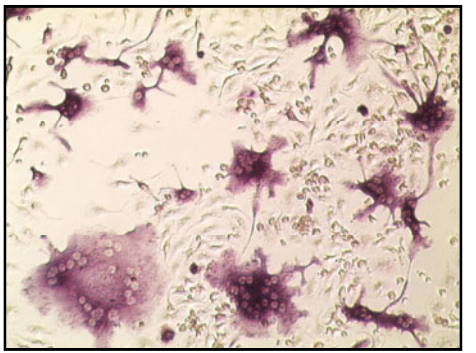

4T1 CM – *abcc5* sh#1

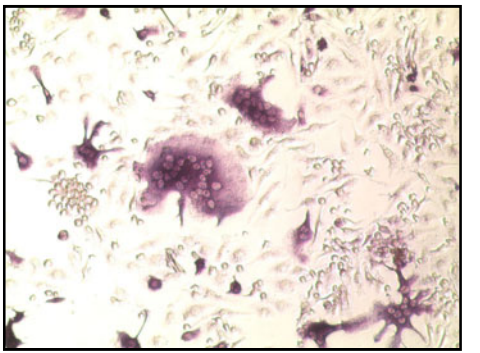

4T1 CM – *abcc5* sh#2

Additional files provided with this submission:

Additional file 1: Additional File 1 - Supplementary M&M.docx, 34K
http://breast-cancer-research.com/imedia/1087239378531864/supp1.docx
Additional file 2: Additional File 2 - Table S1.pdf, 57K
http://breast-cancer-research.com/imedia/1403970185853186/supp2.pdf
Additional file 3: Additional File 3 - Fig. S1.pdf, 1993K
http://breast-cancer-research.com/imedia/1805925953853187/supp3.pdf
Additional file 4: Additional File 4 - Fig. S2.pdf, 2586K
http://breast-cancer-research.com/imedia/2114874908853187/supp4.pdf
Additional file 5: Additional File 5 - Miscoarray Data.xlsx, 6654K
http://breast-cancer-research.com/imedia/2003657208531880/supp5.xlsx
Additional file 6: Additional File 6 - Fig. S3.pdf, 99K
http://breast-cancer-research.com/imedia/3519338718531882/supp6.pdf
Additional file 7: Additional File 7 - Fig. S4.pdf, 391K
http://breast-cancer-research.com/imedia/2012890857853189/supp7.pdf
Additional file 8: Additional File 8 - Fig. S5.pdf, 402K
http://breast-cancer-research.com/imedia/5922681168531906/supp8.pdf
Additional file 9: Additional File 9 - Fig. S6.pdf, 72K
http://breast-cancer-research.com/imedia/1558889926853190/supp9.pdf
Additional file 10: Additional File 10 - Fig. S7.pdf, 32K
http://breast-cancer-research.com/imedia/5406531438531919/supp10.pdf
Additional file 11: Additional File 11 - Fig. S8.pdf, 65K
http://breast-cancer-research.com/imedia/9865840128531911/supp11.pdf
Additional file 12: Additional File 12 - Fig. S9.pdf, 65K
http://breast-cancer-research.com/imedia/6511282785319117/supp12.pdf